Force Feedback Pushing Scheme for Micromanipulation Applications

Shahzad Khan, IEEE Member and Asif Sabanovic, IEEE Senior Member

Abstract— **Pushing micro-objects using point contact provides more flexibility and less complexity compared to pick and place operation. Due to the fact that in micro-world surface forces are much more dominant than inertial forces and these forces are distributed unevenly, pushing through the center of mass of the micro-object may not yield a pure translational motion. In order to translate a micro-object, the line of pushing should pass through the center of friction. In this paper, a semi-autonomous scheme based on hybrid vision/force feedback procedure is proposed to push micro-objects with human assistance using a custom built tele-micromanipulation setup to achieve translational motion. In the semi-autonomous pushing process, velocity controlled pushing with force feedback is realized along x-axis by the human operator while y-axis orientation is undertaken automatically using visual feedback. This way the desired line of pushing for the micro-object is controlled to pass through the varying center of friction. Experimental results are shown to prove nano-Newton range force sensing, scaled bilateral teleoperation with force feedback and snapshot of pushing operation.**

I. INTRODUCTION

As the nature has provided us with things in dimensions ranging down till micro/nanometers likewise humans also were able to fabricate components in the same scales, but the prominent challenge lies in the fact to assemble components in a single and functionalized product. Use of monolithic ways to produce complex micro/nano systems is desirable, but is not always feasible. The current state of art is to incorporate components into a single functional product and to assemble micro parts one by one [1], [2], [3]. The only solution to this problem is to develop setup capable to assist humans to assembly micro-parts. The first and foremost requirement for the assembly process is to "precisely manipulate" objects. Manipulation includes cutting, pushing, pulling, indenting, or any type of interaction which changes the relative position and relation of entities. This paper concentrates on manipulation by pushing as it is a useful technique for manipulating delicate, small, or slippery parts, parts with uncertain location, or parts that are otherwise difficult to grasp and carry [4], [5], [6]. The process of manipulation by pushing of micro-objects possesses many challenges due to the requirements of:

- Actuators with high resolution (in nanometer range), high bandwidth (up to several kilo hertz), large force output (up to few newtons) and relatively large travel range (up to a few millimeters) [7].
- Robust and transparent bilateral controllers for human intervention so that high fidelity position/force interaction between the operator and the remote micro environment can be achieved [8], [9].
- Vision based algorithms to estimate the location of objects being manipulated and visual servoing to position manipulators so that these objects can be pushed along a desired trajectory [10].
- Controlled pushing force to generate the desired compensation surface forces arising between the object and the environment.

Manipulating objects requires not only precise position control of actuators but also delicate control of forces involved in the manipulation process. Visual information is required for path planning whereas use of force feedback is indispensable to ensure controlled physical interactions. Thus, pushing using only visual feedback is not sufficient. It is also indispensable to sense and control the interaction forces involved in the manipulation process with nano-newton resolution. Moreover, it is a well established fact that human operators are much more adaptable to force changes and can react much effectively under unexpected situations as compared other robotic manipulators. In other words, human operator can perform force control and motion operation much more skillfully, thus human intervention can be employed in pushing of the micro-object.

In this paper, vision/force hybrid feedback procedure for force controlled pushing of micro-objects with human assistance is presented. The paper is organized as follows. Section II provides the problem definition and approach and Section III explains the custom built tele-micromanipulation setup. In Section IV, scaled bilateral teleoperation is demonstrated with experimental details concerning force/position tacking between the master and the slave. Finally, Section V provides the procedure for pushing micro-objects along with the experimental results and Section VI concludes the paper and discusses future directions.

II. PROBLEM DEFINITION AND APPROACH

The problem dealt within this work concerns utilizing semi-autonomous manipulation scheme for pushing of polygonal micro-object, by point contact to achieve translational motion with the aid of a human operator employing scaled bilateral teleoperation with force-feedback. In order to achieve translation motion, the proper line of action of the pushing force needs to always pass through the varying center of friction of the polygonal micro-objects. In order to prevent the sliding of the micro-object during the pushing operation, it is necessary that the the pusher falls within the friction cone[1] as denoted in Figure 1. Theoretical value of μ between

[1]friction cone is defined as to be the set of all wrenches satisfying Coulomb's law for an object at rest, i.e. all the wrenches satisfying: $|f_t| \leq \mu |f_n|$

the silicon tip of the cantilever and micro-object is 0.25, thus the angle for friction cone can be calculated as 28.07^o. Thus, while the pushing operation is in progress, it is inevitable to online estimate the center of friction and align the probe such that line of action passes through the center of friction of the micro-object.

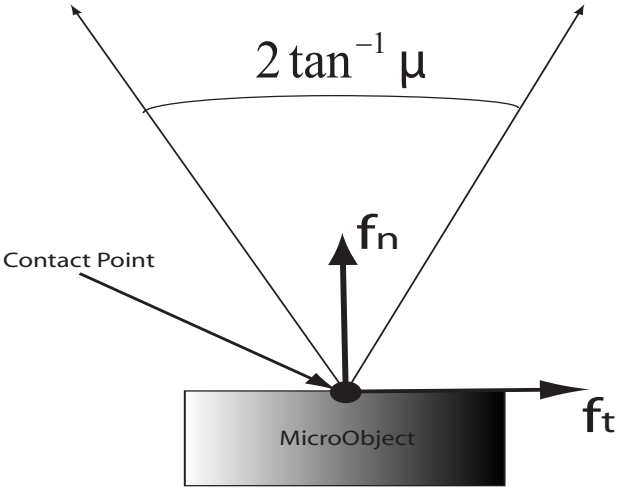

Fig. 1. Friction cone between the pusher and the micro-object

Figure 2 represents the scenario of moving rectangular object using a point contact pushing to achieve pure translation motion. The rectangular micro-object has two points, namely COM (center of mass) and COF (center of friction). The contact point of the pusher is taken as the origin of the reference frame. The x-axis and y-axis of the frame is chosen to be parallel and perpendicular connecting to the edge of polygon. The velocity of the probe along x-axis ($\vec{V}_x$) and y-axis ($\vec{V}_y$) are controlled by visual feedback and human operator, respectively. The desired velocity vector $\vec{V}_{des}$, resultant of $\vec{V}_x$ and $\vec{V}_y$ needs to pass through COF, hence have an angle θ_d to achieve a pure translation motion. The value of $\vec{V}_y$ cannot be controlled to achieve the desired velocity vector as it is administered by the human operator, rather it is only a measurable quantity. The variable $\vec{V}_x$ can be calculated by taking into consideration the value of $\vec{V}_y$ to achieve the desired velocity vector $\vec{V}_{des}$ making an angle θ_d as in the following equations.
The relationship between the $\vec{V}_x$ and $\vec{V}_{des}$ can be written as Eqn.(1) by analyzing Figure 2 and solving for $\vec{V}_{des}$ yields Eqn.(2).

$$\vec{V}_{des}\cos\theta_d = \vec{V}_x \tag{1}$$

$$\vec{V}_{des} = \frac{\vec{V}_x}{\cos\theta_d} \tag{2}$$

Similarly, the relationship between the $\vec{V}_y$ and $\vec{V}_{des}$ can be written as Eqn.(3) and inserting the Eqn.(2) into Eqn.(3) will yield Eqn.(4)

$$\vec{V}_{des}\sin\theta_d = \vec{V}_y \tag{3}$$

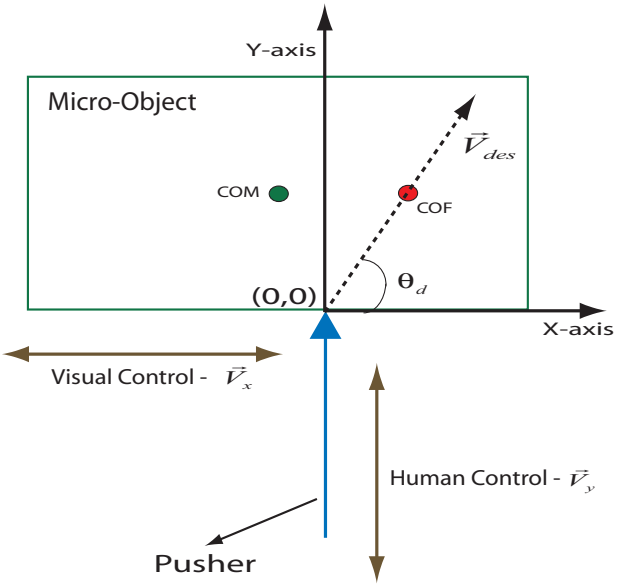

Fig. 2. Calculation of velocity vector for known center of friction

$$\vec{V}_y = \vec{V}_x\tan\theta_d \tag{4}$$

The Eqn.(4) indicates that its possible to only control $\vec{V}_y$ to achieve the resultant velocity vector $\vec{V}_{des}$ to pass through COF.

The whole process of pushing a micro-object is divided into two concurrent process: in one pushing is performed by the human operator which acts as an impedance controller to switch between force-position control and alters the velocity of the pusher while in contact with the micro-object. In the second part, the desired line of pushing for the micro-object is determined continuously by vision based algorithm so that it always passes through the varying center of friction. The necessary subtasks utilized to perform the whole process are as follows:

- Piezoresistive AFM microcantilever has been utilized to measured the interaction forces with the environment with nano-newton resolution.
- Human operator interacts with the micro environment using scaled bilateral teleoperation. The desired position is commanded by the human operator and transferred to the micro environment after scaling and the resultant interaction forces are felt by the human operator after performing the force scaling.
- Visual processing algorithms are employed to detect position and orientation of the micro-object for the estimation of the desired line of pushing.

III. MICROMANIPULATION SETUP

The system is composed of three parts, namely human-bilateral system, vision system and XYZ manipulator as shown in Figure 3.
The position data from the master side is scaled and transferred to slave side, while simultaneously, the force measured at the slave side is scaled and transferred back to master.

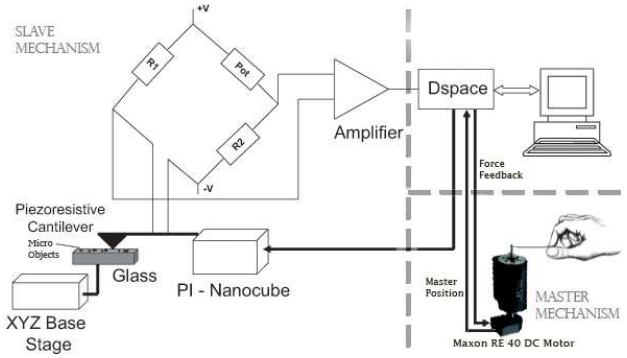

Fig. 3. Schematic of tele-micromanipulation system.

Figure 4 shows the experimental setup. The modules which has been utilized for different functionality are as follows:

- As a 1DOF master device, DC servo (Maxon Motor RE40) has been utilized along with the light rod connected with the shaft.
- In order to move the cantilever with high precision, three axes Piezo stages P-611 by Physik Instrumente has been utilized as a fine motion.
- An open loop piezoelectric micrometer drive (PiezoMike PI-854 from Physik Instrumente) has been utilized as the base stage, which is equipped with integrated high resolution piezo linear drives.
- For nano-wenton range force sensing, a piezoresistive AFM cantilever (from AppNano) has been utilized along with a inbuilt Wheatstone bridge.
- A real time capable control card dSPACE DS1103 is used as control platform and the programming is done in C.
- For visual feedback, Nikon MM-40 Microscope along with two Unibrain Fire-i 400 FireWire camera is connected to the microscope to capture the visual data and send to computer.

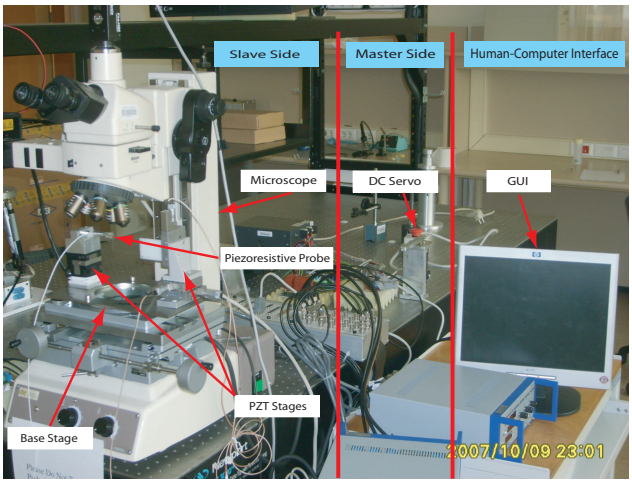

Fig. 4. Experimental setup for micromanipulation

IV. SCALED BILATERAL TELEOPERATION

In this section implementation of scaled bilateral control in a custom built tele-micromanipulation setup is presented. Force sensing with nN resolution using piezoresistive AFM (Atomic Force Microscope) micro-cantilever is demonstrated. Force/position tracking and transparency between the master and the slave is presented with varying references after necessary scaling.

A. Force Sensing Using Piezoresistive AFM Microcantilever

Piezoresistive AFM cantilever with inbuilt Wheatstone bridge from AppliedNanostructures is utilized as a force sensor as well as probe for pushing operation.

The working principle is based on the fact that as the force is applied at the free end of the cantilever using the PZT actuator with the glass slide, the change of resistance takes place depending on deflection of the cantilever. The amount of deflection is measured by the in-built Wheatstone bridge providing a voltage output, which is amplified by the custom built amplifier. The amplified voltage is send to the data acquisition dSpace1103 card for further processing.

1) Experimental Results for Force Sensing: Figure 5 [10], [11] represents the attractive forces for pulling in phase between the tip and glass slide. The decreasing distance between the tip and glass slides is represented by the increase in the position of PZT axis. As the distance between the tip and glass slide decreases the attractive forces increases. The result clearly indicates that force sensing with the resolution of nN range is achieved.

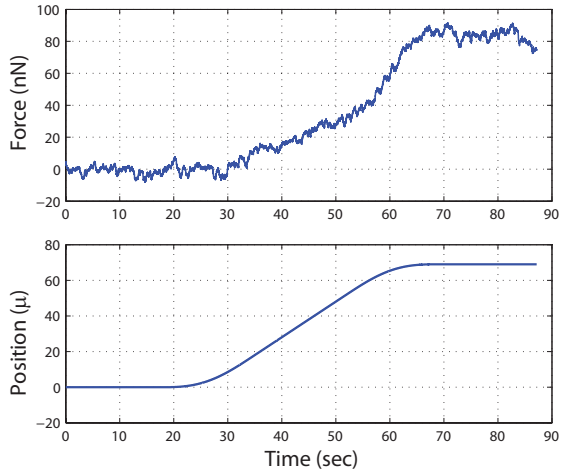

Fig. 5. Force for smooth step position reference.

B. Scaled Bilateral Control Structure

Since the master and slave are working on macro and micro scales respectively, thus its indispensable to use general bilateral controller to scale the position and forces between two sides for extensive capability [12]. In other words, position information from the master is scaled down to slave and force information from the slave side in scaled up to master as shown in Figure 6 comprising of the

master and the slave side. Piezo-stage on the slave side is required to track master's position as dictated by position controller. The $1D$ force of interaction with environment, generated by piezoresistive cantilever, on the slave side is transferred to the master as a force opposing its motion, therefore causing a "feeling" of the environment by the operator. The conformity of this feeling with the real forces is called the "transparency". Transparency is crucial for micro/nanomanipulation application for stability of the overall system.

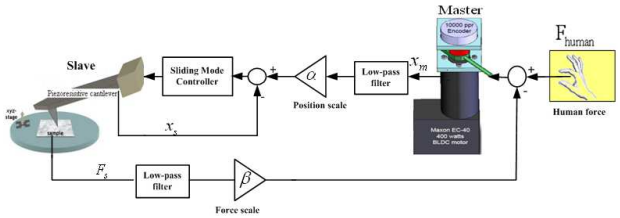

Fig. 6. Scaled bilateral teleoperation control structure

In order to eliminate oscillations on master side because of oscillatory human hand and on the slave side due to piezoresistive cantilever dynamics, position of master manipulator and force of slave manipulator are filtered by low pass filters before scaling.

1) Scaling of the Position and Force Information: Since the master and slave side resides on macro and micro scales respectively, thus its very vital to appropriately choose the scaling factor in order to attain the optimum performance. In the ideal condition, the steady state condition of the bilateral controller should be Eqn.(5).

$$\begin{aligned} x_s &= \alpha x_m \\ F_m &= \beta F_s \end{aligned} \tag{5}$$

Where α and β represents the position and force scaling respectively. x_m,x_s denotes the master and slave position respectively and F_m, F_s denotes the master and slave force respectively. To be able to meaningfully interact with the micro environment, positions and forces are scaled to match the operator requirements.

In the first and second experiments, scaling factors of $\alpha = 0.027\frac{\mu m}{deg}$ and $\beta = 0.00366\frac{N}{nN}$ are used, that is an angular displacement of $1deg$ on the master side corresponds to a linear displacement of $0.027\mu m$ on the slave side and a force of $0.00366nN$ on the slave side corresponds to a force of $1N$ on the master side. The objective of these experiments is to provide very fine motion on the slave side for a relatively larger displacement on the master side, hence α is selected according to this objective. Then the corresponding forces/torques for each amount of displacement were compared for the selection of β, keeping in mind that the DC motor on the master side has low torques.

2) Experimental Validation for Force/Position Tracking: In order to validate the position tracking between the master and the slave, the commanded position from the master is transferred after necessary scaling to be tracked by the slave side. Figure 7 illustrates the experimental results for position tracking along with the tracking error of the bilateral controller. It can be clearly seen that the slave tracks the master position with high accuracy. This position tracking performance is acceptable for precisely positioning the micro cantilever.

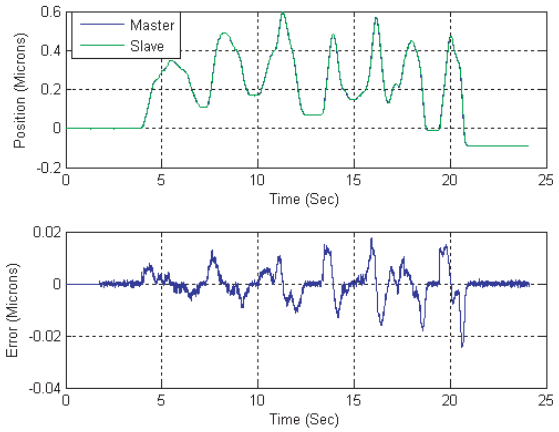

Fig. 7. Position Tracking between the master and the slave

In order to validate the force tracking, the slave forces encountered from the environment is being transferred to the master side after necessary scaling. Figure 8 demonstrates the force tracking between the master and slave along with the tracking error. It can be clearly observed that the master tracks the slave force precisely.

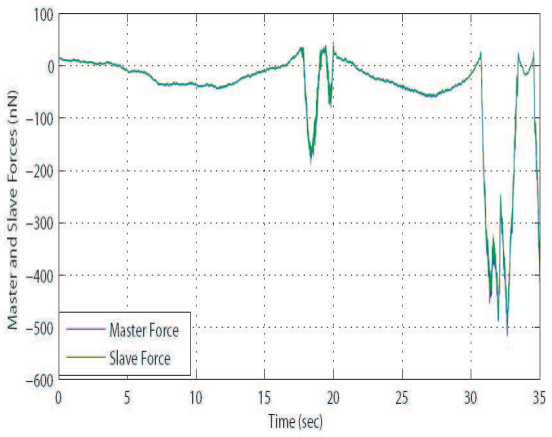

Fig. 8. Force tracking between the master and the slave

V. SEMI-AUTONOMOUS PUSHING SCHEME

A. Point Contact Pushing For Translational Motion

Precise positioning of micro-objects lying on a substrate using a point contact pushing to track a desired trajectory posses lot of challenges. The pusher or probe needs to controlled in such a way to reorient and transport the microobject to its final location using a stable pushing operation. Using only a point contact with a limited number of freedom

the task of pushing on a horizontal plane can be realized. Pushing in micro domain is heavily dominated by the varying frictional distribution which can be lumped at a single point as center of friction. Thus, the resulting line of pushing needs to be directed through center of friction to achieve translational motion [13].

B. Center of Friction

In this subsection, the focuss is on the estimation of the center of friction of the rectangular micro-object lying on a support surface and pushed by the point contact probe using the technique proposed by Yoshikawa [14]. However, the concept is further extended by online estimation of COF for each visual data and necessary value of θ_d is updated online.

Some of the assumption which needs to considered are as follows:

1) The micro-object is rigid.
2) The micro-object is in contact with the supporting surface with n points. In this case n=4, as the four corners of the rectangle.
3) The position of the supporting points with respect to the object remains unchanged even when the micro-object is in motion.
4) Since the micro-object is pushed by point contact, the friction between the pusher and micro-object is assumed to be negligible due to the fact that contact area is very small.
5) The coefficient of friction between the object and the support surface may depend on the position of the supporting point, but is constant with respect to time.
6) The pushing force is applied horizontally to a point on the object near the support surface.
7) The inertial force can be ignored in comparison with the frictional force.

Figure 9 represents the micro-object lying on the supporting surface. A reference coordinate frame $\sum_u(O_u - X_uY_uZ_u)$ is attached to the supporting surface. An object coordinate frame $\sum_o(O_o - X_oY_oZ_o)$ is also fixed to the object with its X_0Y_0 plane coinciding the base of the object. Some of the notations expressed in $\sum_0$ are defined as follows:

- p_i : Position of i^{th} supporting point.
- v_i : Velocity of object relative to support surface at p_i.
- a_i : Magnitude of frictional force at p_i.
- f_i : Frictional force at p_i.
- f : Frictional force vector.
- m_i : Frictional moment at p_i with respect to $\sum_0$.
- F_f : Total frictional force.
- M_f : Total frictional moment with respect to $\sum_0$.
- F_c : The pushing force applied by the probe.
- p_c : The location of the contact point with the micro-object.
- p_g : The location of the center of friction.

The frictional force f_i and the frictional moment m_i at the i^{th} supporting point are given by, Eqn.(6) and Eqn.(7), respectively:

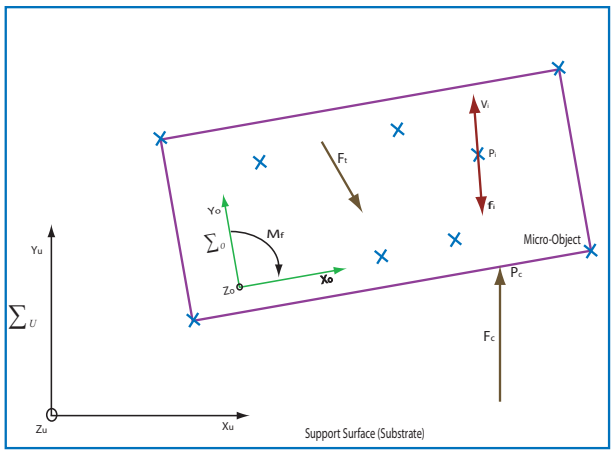

Fig. 9. Reference frame and object frame

$$f_i = -\frac{v_i}{\|v_i\|}a_i \tag{6}$$

$$m_i = p_i \times -\frac{v_i}{\|v_i\|}a_i \tag{7}$$

where $\|.\|$ and $\times$ denote the Euclidean norm and the vector product. Thus, the total frictional F_f and total frictional moment M_f can be represented in Eqn.(8) and Eqn.(9), respectively:

$$F_i = \sum_{i=1}^{n} f_i = -\sum_{i=1}^{n} \frac{v_i}{\|v_i\|}a_i \tag{8}$$

$$M_f = \sum_{i=1}^{n} m_i = -\sum_{i=1}^{n} \left\{p_i \times \frac{v_i}{\|v_i\|}a_i\right\} \tag{9}$$

If the micro-object rotates, then the position of instantaneous center of rotation of the motion $p_r = [x_r, y_r, 0]^T$ can be deduced by using visual data. In Figure 10 the origin of the reference frame is place at the lower left vertex of the rectangle. The edges PQ and P′Q′ are the two edges of the rectangular micro-object before and after pushing by a probe using point contact. The midpoints of the line PP′ and QQ′ are found and a perpendicular line is formed from both the midpoints. The point where the two lines intersect meet is the instantaneous center of rotation referred as p_r whose location is denoted as $[x_r, y_r, 0]^T$.

The unit vector which is along the direction of relative velocity at each supporting point $p_i = [x_i, y_i, 0]^T$ is denoted in Eqn.(10).

$$\frac{v_i}{\|v_i\|} = k \times \frac{p_i - p_r}{\|p_i - p_r\|} \tag{10}$$

where k is the unit vector that is along the direction of the rotation of the object. Let the rotational angle of frame $\sum_0$ with respect to $\sum_u$ be θ. The unit vector k can be calculated as k is $[0, 0, sgn(\theta)]^T$. The value of $k = [0, 0, -1]^T$ when the direction of rotation is counterclockwise and $k = [0, 0, 1]^T$ when its object is rotating clockwise. The pushing force F_c

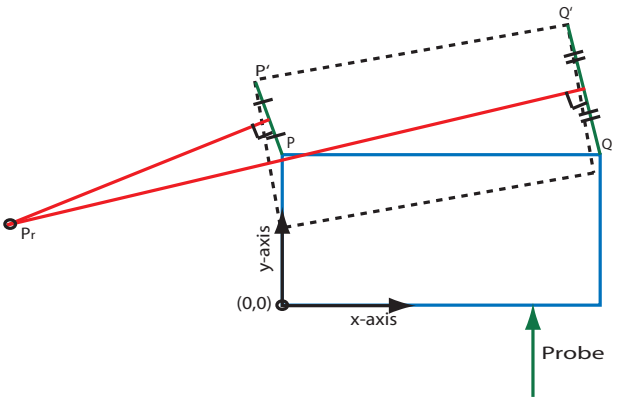

Fig. 10. Instantaneous center of rotation

at the contact point $p_c = [x_c, y_c, 0]$ can be decomposed as $F_c = [F_{cx}, F_{cy}, 0]^T$ and with assumption 7, one can state the following relations;

$$F_c = -F_f \tag{11}$$

$$M_c = -M_f = p_c \times F_c \tag{12}$$

where $M_c = [0, 0, M_{cz}]^T$ denotes the moment due to F_c. Let the total friction force F_f be decomposed of $F_f = [F_{fx}, F_{fy}, 0]^T$, $M_f = [0, 0, M_{fz}]^T$. From the Eqs.(8−12), one can obtain Eqs.(13−15).

$$sgn(\dot{\theta})F_{cx} = -\sum_{i=1}^{n} \frac{Y_i}{R_i} a_i \tag{13}$$

$$sgn(\dot{\theta})F_{cy} = \sum_{i=1}^{n} \frac{X_i}{R_i} a_i \tag{14}$$

$$sgn(\dot{\theta})M_{cz} = \sum_{i=1}^{n} \frac{x_i X_i + y_i Y_i}{R_i} a_i \tag{15}$$

Then, the value of X_i, Y_i and R_i can be expressed as

$$X_i = x_i - x_r, Y_i = y_i - y_r, R_i = \sqrt{X_i^2 + Y_i^2} \tag{16}$$

Since a_i is the magnitude of the frictional force at the supporting point (x_i, y_i), a frictional force vector can be formed as $f = [a_1, a_2...., a_n]^T$ for n supporting points. If the object moves without any rotation, the direction of the relative velocity $\frac{v_i}{\|v_i\|}$ of all the supporting point are the same and can be written as

$$e_v = \frac{v_i}{\|v_i\|}, (i = 1, 2..., n) \tag{17}$$

Rewriting the value of F_f and M_f, one can derive

$$F_f = -e_v \sum_{i=1}^{n} a_i \tag{18}$$

$$M_f = -\Big\{ \sum_{i=1}^{n} p_i a_i \Big\} \times e_v \tag{19}$$

Define a variable p_g and represented as if

$$p_g = \frac{\sum_{i=1}^{n} a_i p_i}{\sum_{i=1}^{n} a_i} \tag{20}$$

By the definition of p_g, Eqn.(19) can be written as

$$M_f = p_g \times F_f \tag{21}$$

Eqn.(21) indicates the total frictional force F_f to cause a frictional moment of M_f acts on the objects at point p_g, called as center of friction. From Eqn.(11) and Eqn.(18), the pushing force applied to the micro-object can be written as

$$F_c = e_v \sum_{i=1}^{n} a_i \tag{22}$$

$$\begin{aligned} M_c + M_f &= 0 \\ \overrightarrow{p_c} \times \overrightarrow{F_c} + \overrightarrow{p_g} + \overrightarrow{F_f} &= 0 \\ (\overrightarrow{p_c} - \overrightarrow{p_g})\overrightarrow{F_c} &= 0 \\ \overrightarrow{p_g} &= \overrightarrow{p_c} \end{aligned} \tag{23}$$

By analyzing Eqn.(22) and Eqn.(23), it can be concluded for a translational motion that the direction of F_c needs to be the same as the motion of the object and the line of action of F_c needs to pass through p_g. In other words, if one applies a external force F_c acting on the object such that the line of action F_c passes through the point p_g, then it is possible to push the object without any rotation.

C. Method for Online Estimation of the Center of Friction

The change in the location of the COF may be very fast,thus online estimation of COF needs to be performed and the probe needs to align so that the line of action of the applied force F_c passes through the COF.

Visual information is utilized to determine the position and velocities of the four corners, the centroid of mass for the rectangular micro-object along with the position of the contact point $p_c = (x_c, y_c)$ with the probe. The instantaneous center of rotation p_r and orientation angle θ are calculated using image processing techniques. The force F_c measured by the probe can be decomposed into two dimension as $F_{cx} = F_c cos\theta$ and $F_{yx} = F_c sin\theta$, where θ is the orientation angle. The moment M_{cz} generated by the applied force be written as

$$M_{cz} = x_c F_{cy} - y_c F_{cx} \tag{24}$$

The relationship between the pushing force F_c and frictional force vector f which can be written as

$$F_c = Gf \tag{25}$$

where F_c is calculated for each two consecutive frames captured using as

$$
\begin{aligned}
F_c &= [sgn(\dot{\theta}_1)F_{cx1}, sgn(\dot{\theta}_1)F_{cy1}, \\
&\quad sgn(\dot{\theta}_1)M_{cz1}, sgn(\dot{\theta}_1)F_{cx2}, \\
&\quad sgn(\dot{\theta}_2)F_{cy2}, sgn(\dot{\theta}_2)M_{cz2}]^T
\end{aligned} \tag{26}
$$

where F_{cx1}, F_{cy1}, M_{cz1} represent pushing force in x-axis for the first captured frame, pushing force in y-axis for the first captured frame and moment in the z-direction for the first captured frame respectively. Similarly F_{cx2}, F_{cy2}, M_{cz2} represents for the second captured frame. The value of $G_{4\times 6}$ matrix is calculated using two sets of consecutive captured frame and four supporting points considering the vertices of the rectangle. The $G_{4\times 6}$ is written as

$$
G = \begin{bmatrix}
-\frac{Y_{11}}{R_{11}} & -\frac{Y_{21}}{R_{21}} & -\frac{Y_{31}}{R_{31}} & -\frac{Y_{41}}{R_{41}} \\
\frac{X_{11}}{R_{11}} & \frac{X_{21}}{R_{21}} & \frac{X_{31}}{R_{31}} & \frac{X_{41}}{R_{41}} \\
\frac{x_1X_{11}+y_1Y_{11}}{R_{11}} & \frac{x_2X_{21}+y_2Y_{21}}{R_{21}} & \frac{x_3X_{31}+y_3Y_{31}}{R_{31}} & \frac{x_4X_{41}+y_4Y_{41}}{R_{41}} \\
-\frac{Y_{12}}{R_{12}} & -\frac{Y_{22}}{R_{22}} & -\frac{Y_{32}}{R_{32}} & -\frac{Y_{42}}{R_{42}} \\
\frac{X_{12}}{R_{12}} & \frac{X_{22}}{R_{22}} & \frac{X_{32}}{R_{32}} & \frac{X_{42}}{R_{42}} \\
\frac{x_1X_{12}+y_1Y_{12}}{R_{12}} & \frac{x_2X_{22}+y_2Y_{22}}{R_{22}} & \frac{x_3X_{32}+y_3Y_{32}}{R_{32}} & \frac{x_4X_{42}+y_4Y_{42}}{R_{42}}
\end{bmatrix} \tag{27}
$$

From Eqn.(26), an estimate value of $f(\hat{f})$ can be derived as

$$
f = G^+F \tag{28}
$$

where G^+ is the pseudo-inverse matrix of G matrix. From Eqn.(20), the estimated location of the center of friction $\hat{p_g}$ can be obtained as

$$
\hat{p_g} = \frac{X^T\hat{f}}{e_n^T\hat{f}} = \frac{X^TG^+F}{e_n^TG^+F} \tag{29}
$$

where X^T represents the location of each vertices of the rectangle and can be written in matrix form as

$$
X = \begin{bmatrix}
x_1 & x_2 & x_3 & x_4 \\
y_1 & y_2 & y_3 & y_4 \\
0 & 0 & 0 & 0
\end{bmatrix}^T \tag{30}
$$

where e_n represents unity vector with four elements as

$$
e_n = [1, 1, 1, 1]^T \tag{31}
$$

D. Pushing Algorithm

The pushing operation is performed in several steps as follows:

- Step 1: Aligning the micro-cantilever such that the probe is in contact with micro-object at the midpoint of the length using the bilateral teleoperation as discussed in Section IV.
- Step 2: Human operator starts to push the object using bilateral teleoperation and monitors the behavior of the object using visual display. Concurrently, the visual processing generate the position and velocities of vertexes and contact point.
- Step 3: The data from visual processing is utilized to calculate the center of rotation p_r and concurrently the force exerted F_c by the probe is utilized to calculate F_{cx}, F_{cy} and M_{cz}.
- Step 4: The matrix F_c and G are formed using two successive visual and force data sets. The force data is downsampled and averaged to 30 Hz to matching the sampling rate of visual frame capturing.
- Step 5: The value of the center of friction p_g is estimated using the values obtained in Step 4 and thereafter desired value of the velocity of the probe in x-direction $\vec{V_x}$ is calculated so that the vector of the resultant can be orientated to ensure that the line of action passes through the estimated center of friction.
- Step 6: $\vec{V_x}$ is set to the calculated value and kept constant until the arrival of new visual data.
- Step 7: The human operator continuously monitors any sliding of the micro-object at the contact point which may result if the probe comes out of the friction cone. When sliding occurs, the human operator reverts back and changes the location of the contact point after rotation stages is orientated to proper value.
- Step 8: Step 3 is repeated using the next visual data and the first three rows of G matrix are updated each time new data sets becomes available. Step 3 to Step 6 are repeated in a recursive manner to track the location of the center of friction.

Human operator is responsible for generating desired force for pushing of the micro-object by visualizing the motion of the micro-object and can pull the probe back if undesirable behavior in the motion of the micro-object is observed during any of the above mentioned steps. Since humans are very good at adapting to unexpected change in the forces, the force controlled pushing operation is administered by human operator.

E. Experimental Validation of Pushing Operation

In order validate the above mentioned pushing algorithm, several experiments were conducted by pushing a rectangular micro-object of size $200\ \mu m$ at the mid-point of the length of rectangle and the line of action passes through the center of mass. Figure 11 demonstrates the snapshot of the pushing operation and it can be clearly observed that after several steps the micro-object starts to rotate. Thus, it is unmanageable to translate a micro-object by pushing through the center of mass.

The above results shows that to achieve pure translation motion it is necessary that the line of action passes through the center of friction to compensate the orientation angle. Figure 12 demonstrates the snapshot of pushing rectangular micro-object such that the line of action passes through the center of friction. Figure 13 shows the position of Y-axes and forces during pushing operation. It can be clearly seen that the proposed procedures was able to compensate the orientation effect to attain pure translational motion.

VI. CONCLUSIONS

In this paper, a semi-autonomous scheme based on hybrid vision/force feedback using a custom built tele-micromanipulation is proposed. The pushing operation is undertaken by the human operator using visual display which

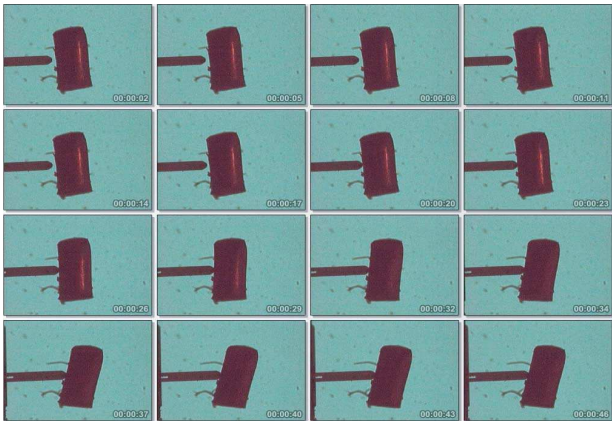

Fig. 11. Snapshot of pushing rectangular object at the mid-point of the rectangle and line of action passes through center of mass of the object.

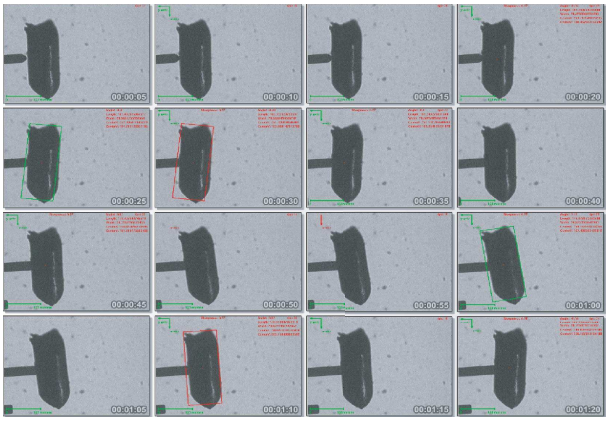

Fig. 12. Snapshot of pushing rectangular object such that the line of action passes through the center of friction

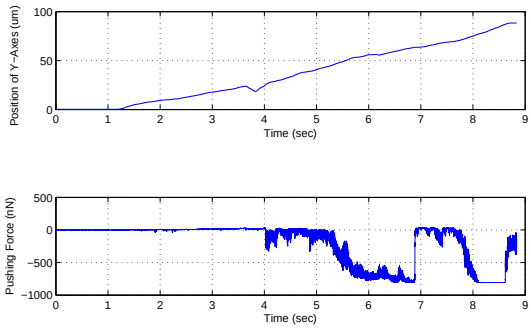

Fig. 13. Top represents the position of Y-axes and bottom figure shows the pushing force.

acts an impedance controller and can switch between velocity control to force control by adjusting the stiffness (muscle stiffness) depending upon the behavior of the motion of the micro-object. Visual module provides the information about the position and orientation of the micro-object to calculate the time-varying COF (center of friction) in recursive manner for each captured frame. The velocity at the contact point is altered using visual feedback procedures such that the resultant direction of velocity passes through the COF to achieve pure translational motion. Experimental results concerning nano-newton resolution force sensing, force/position tracking between the master and the slave is presented which is a requirement to fulfill the pushing operation.

VII. ACKNOWLEDGMENTS

The authors gratefully acknowledge the financial contributions by TUBITAK, Ankara and Yousef Jameel Scholarship.

REFERENCES

[1] N. Dechev, W. L. Cleghorn, and J. K. Mills, "Construction of 3d mems microcoil using sequential robotic microassembly operations," in *ASME International Mechanical Engineering Congress*, 2003.

[2] K. Furuta, "Experimental processing and assembling system (micro-factory)," in *International Micromachine Symposium*, pp. 173–177, 1999.

[3] D. O. Popa and H. E. Stephanou, "Micro and meso scale robotic assembly," in *WTEC Workshop: Review of U.S. Research in Robotics*, 2004.

[4] K. M. Lynch and M. T. Mason, "Stable pushing: Mechanics, controllability, and planning," *The International Journal of Robotics Research*, vol. 15, no. 6, pp. 533–556, 1996.

[5] K. M. Lynch, "Locally controllable manipulation by stable pushing," *IEEE Transactions on Robotics and Automation*, vol. 15, no. 2, pp. 318–327, 1999.

[6] M. Sitti, "Atomic force microscope probe based controlled pushing for nano-tribological characterization," *IEEE/ASME Transactions on Mechatronics*, vol. 8, no. 3, 2003.

[7] S. Khan, M. Elitas, E. D. Kunt, and A. Sabanovic, "Discrete sliding mode control of piezo actuator in nano-scale range," in *IIEEE/ICIT International Conference on Industrial Technology*, 2006.

[8] M. Sitti and H. Hashimoto, "Teleoperated touch feedback from the surfaces at the nanoscale: Modeling and experiments," in *IEEE/ASME Transactions on Mechatronics*, vol. 8 of *1*, pp. 287–298, 2003.

[9] T. Tsuji, K. Natori, and K. Ohnishi, "A controller design method of bilateral control system," in *European Power Electronics Power Electronics and Motion Control Conference*, vol. 4, pp. 123–128, 2004.

[10] S. Khan, A. O. Nergiz, A. Sabanovic, and V. Patoglu, "Development of a micromanipulation system with force sensing," in *IEEE/IROS International Conference on Intelligent Robots and Systems*, 2007.

[11] S.Khan, A.Sabanovic, and A.O.Nergiz, "Scaled bilateral teleoperation using discrete-time sliding mode controller," in *IEEE Transaction in Industrial Electronics*, p. Accepted, 2007.

[12] M.Elitas, S.Khan, A.Sabanovic, and A.O.Nergiz, "Function based control of constrained motion systems for microsystems applications," in *IEEE Transaction in Industrial Electronics*, 2008 (In Review).

[13] M.T.Mason, "Mechanics and planning of manipulator pushing operations," in *International Journal of Robotics Research*, vol. 5 of *3*, pp. 53–71, 1986.

[14] T. Yoshikawa and M. Kurisu, "Identification of the center of friction from pushing an object by a mobile robot," in *IEEE/RSJ International Workshop on Intelligent Robots and Systems - IROS*, 1991.